

Time-of-flight observables and the formation of Mott domains of fermions and bosons on optical lattices

M. Rigol,¹ R. T. Scalettar,¹ P. Sengupta,² and G. G. Batrouni³

¹*Physics Department, University of California, Davis, CA 95616, USA*

²*Department of Physics, University of Southern California, Los Angeles, CA 90089, USA*

³*Institut Non-Linéaire de Nice, UMR 6618 CNRS,*

Université de Nice-Sophia Antipolis, 1361 route des Lucioles, 06560 Valbonne, France

We study, using quantum Monte Carlo simulations, the energetics of the formation of Mott domains of fermions and bosons trapped on one-dimensional lattices. We show that, in both cases, the sum of kinetic and interaction energies exhibits minima when Mott domains appear in the trap. In addition, we examine the derivatives of the kinetic and interaction energies, and of their sum, which display clear signatures of the Mott transition. We discuss the relevance of these findings to time-of-flight experiments that could allow the detection of the metal–Mott-insulator transition in confined fermions on optical lattices, and support established results on the superfluid–Mott-insulator transition in confined bosons on optical lattices.

PACS numbers: 03.75.Ss, 05.30.Fk, 05.30.Jp, 71.30.+h

Following the successful loading of ultracold Bose gases on optical lattices,^{1,2} a similar scenario has been achieved in recent experiments with ultracold fermions.^{3,4,5,6} In Refs. 3 and 4 an optical lattice was superposed on highly anisotropic traps to study transport properties and localization effects in ideal Fermi gases and Bose–Fermi mixtures. More recently, Hubbard- and Luttinger-type systems have been realized by loading fermionic atoms on three-⁵ and two-dimensional⁶ optical lattices, respectively. Now that such experimental setups are available, one of the most prominent goals is the achievement of the metal–Mott-insulator transition⁷ in confined fermions on optical lattices.^{8,9}

Ultracold fermions on optical lattices are an almost ideal realization of the Hubbard model, in which all parameters can be controlled with very high precision. In this work, we are interested in the one-dimensional (1D) regime,^{2,6} where the Hamiltonian can be written as

$$H = -t \sum_{i,\sigma} \left(c_{i\sigma}^\dagger c_{i+1\sigma} + c_{i+1\sigma}^\dagger c_{i\sigma} \right) + U \sum_i n_{i\uparrow} n_{i\downarrow} + V_2 \sum_i x_i^2 n_i, \quad (1)$$

where $c_{i\sigma}^\dagger$, $c_{i\sigma}$ are the creation and annihilation operators of a fermion in a pseudospin state σ at site i (and position x_i), and $n_i = \sum_\sigma n_{i\sigma}$ ($n_{i\sigma} = c_{i\sigma}^\dagger c_{i\sigma}$) is the particle number operator. The on-site interaction parameter is denoted by U ($U > 0$), the hopping amplitude by t , and V_2 is the curvature of the harmonic confining potential. In experiments, t and U can be modified by changing the intensity of the laser beams that produce the lattice. In addition, U can be also controlled separately by means of a Feshbach resonance,^{5,6} which is the mechanism we consider below. Our quantum Monte Carlo (QMC) simulations of the fermionic Hubbard model were performed using a projector algorithm^{10,11} along the lines described in Refs. 8 and 9.

In the absence of a confining potential ($V_2 = 0$), the phase diagram of this model, Eq. (1), for $U > 0$, consists of a Mott-insulating (MI) phase at half-filling ($n = 1$), trivial band insulating phases for $n = 0, 2$, and a metallic phase for any other density. In the presence of a confining potential $V_2 \neq 0$, these phases coexist in space separated regions.^{8,9} Local measurements may then provide an experimental proof of the existence of MI domains in the trap.^{8,9} A recent proposal¹² also includes collective oscillations as a possible way to detect their formation. However, the demonstration of the MI for fermions is more difficult than in the bosonic case. This is because the appearance of Mott regions for bosons can be detected experimentally by means of standard time-of-flight (TOF) measurements,^{1,2} while in the fermionic case the momentum distribution does not exhibit any distinguishing feature when MI plateaus develop in the trap.⁹

We propose here a novel way to detect the metal–MI transition in fermionic systems. We find that the sum of kinetic and interaction energies, which can be measured in TOF experiments, and their numerical derivatives show distinctive signatures of the formation of Mott domains of fermions as well as bosons trapped on optical lattices. Hence, energy measurements provide a unified way to deal with the Mott transition in confined atoms (fermions or bosons) on optical lattices.

Bosons on 1D optical lattices can be described by the boson Hubbard model¹³

$$H = -t \sum_i \left(a_i^\dagger a_{i+1} + a_{i+1}^\dagger a_i \right) + \frac{U}{2} \sum_i n_i (n_i - 1) + V_2 \sum_i x_i^2 n_i, \quad (2)$$

where a_i^\dagger , a_i are the creation and annihilation operators of a bosonic atom at site i , and $n_i = a_i^\dagger a_i$ is the particle number operator. The hopping parameter, on-site interaction, and curvature of the confining potential are de-

noted as in the fermionic case. The QMC simulations of the boson Hubbard model were done using the stochastic series expansion (SSE) method¹⁴ in the grand canonical ensemble in which an additional chemical potential term in Eq. (2) is used to control the filling.

In Fig. 1(a), we show the evolution of the variance of the density ($\Delta_i = \langle n_i^2 \rangle - \langle n_i \rangle^2$) in a 1D system of fermions when the on-site repulsion is increased using a Feshbach resonance. At $U = 0$, $n_i < 2$ throughout the trap so that no local “band insulator” is present. This can be easily checked experimentally measuring the momentum distribution function, which should exhibit a Fermi momentum k_F , i.e., $n_{k > k_F} = 0$.¹⁵ (The band insulator always produces a finite occupation of all momentum states within the Brillouin zone.)¹⁵ For $U > 4t$, a region of small Δ_i , indicating suppressed (but finite) quantum fluctuations of the density, appears in the center of the trap showing the establishment of a MI there.^{8,9} Notice that in a trap, in contrast to periodic systems at half-filling, the MI appears only for a finite value of U/t .

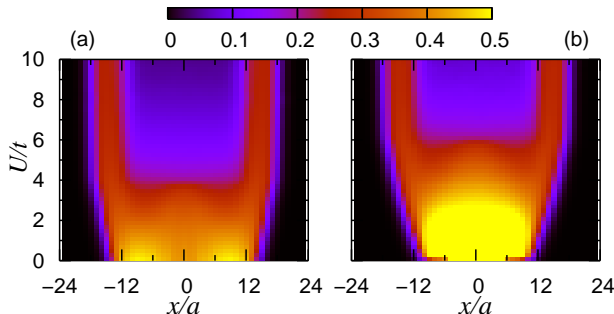


FIG. 1: (color online). Intensity plot of the density fluctuations $\Delta_i = \langle n_i^2 \rangle - \langle n_i \rangle^2$ vs position and interaction strength, in fermionic (a) and bosonic (b) systems with 30 atoms on 48 lattice sites and $V_2 a^2 = 0.015t$ (a is the lattice constant). The lattice size was chosen large enough so that the particle density is zero at the boundaries. For large U , the constant small value of Δ_i in the center of the trap signals the formation of the MI core. In (b), for low values of U/t , we have truncated Δ_i at 0.5, i.e., for low on-site repulsive interactions the bosonic fluctuations of the density exceed 0.5.

The corresponding evolution of Δ_i , for a bosonic system with the same trap parameters and number of particles as the fermionic case, Fig. 1(a), is depicted in Fig. 1(b). Δ_i again signals the formation of a MI plateau¹⁷ when $U \sim 6.1t$, i.e., a value that is $\sim 2t$ larger than in the fermionic case and also larger than the critical value $U/t = 3.5$ in the periodic case.¹⁶ Although for small values of U , quantum fluctuations of the density for bosons are much larger than for fermions (in the figure we have truncated them at $\Delta = 0.5$), when U is increased both systems behave analogously, revealing the similarities between bosons and fermions in 1D.

Several approaches based on TOF measurements have been followed in experiments to detect the formation of Mott domains of bosons. They include the disappearance of the interference pattern,¹ the increase of the full width

at half maximum,^{2,18,19} and more recently the behavior of the visibility.^{20,21} They are all related to the momentum distribution function n_k of the trapped system, which is measured in TOF experiments. We have studied these observables in the fermionic case, and found no signature of the formation of MI domains.

A further quantity related to n_k that can be also obtained experimentally is the kinetic energy,

$$E_K = -2t \sum_k n_k \cos(ka), \quad (3)$$

where a is the lattice parameter, and $-2t \cos(ka)$ is the lattice dispersion relation.

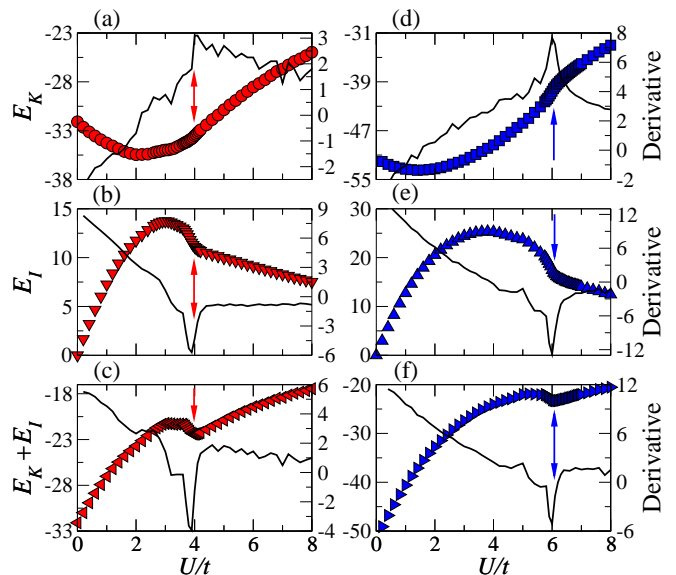


FIG. 2: (color online). (a), (d) Kinetic energy (E_K), (b), (e) interaction energy (E_I), and (c), (f) the sum $E_K + E_I$, for fermions (a-c) and bosons (d-f) in the systems of Fig. 1 (30 atoms and $V_2 a^2 = 0.015t$). Energies are given in units of t . Continuous lines depict numerical derivatives of the energies. The arrows signal the emergence of a MI core. The QMC errors are much smaller than our symbol sizes throughout this work.

The evolution of the kinetic energy with U , for the fermionic system in Fig. 1, is shown in Fig. 2(a). E_K does not exhibit any special feature at the point where the MI appears in the system. In contrast, the interaction energy (E_I), depicted in Fig. 2(b), displays a sharp drop just before the Mott plateau sets in. After that, the decrease of E_I occurs slowly, even more slowly than the reduction of the modulus of the kinetic energy. This suggests that if one turns the trap off and lets the particles expand on the lattice, so that the interaction energy is converted to kinetic energy, the resulting kinetic energy $E'_K = E_K + E_I$ can be used to determine when the MI forms. Figure 2(c) shows that E'_K exhibits a local minimum where the Mott core appears in the system.

An enhanced signal of the features observed in E_I and $E_I + E_K$ can be obtained by calculating their numerical

derivatives. As shown in Figs. 2(b) and 2(c), a large reduction in the derivatives of both quantities occurs just before the MI sets in the center of the trap. The minimum in $E_I + E_K$ is signaled by a vanishing derivative. The derivative of the kinetic energy, Fig. 2(a), exhibits another signal, a weak maximum and a steady decrease after the formation of the MI core.

Using a Feshbach resonance, one can also obtain a final E'_K exhibiting the features observed in E_I , Fig. 2(b). To that end, just before turning off the trap, one could increase U (and hence E_I) by a large constant factor, in a timescale much smaller than the scale set by the hopping parameter (\hbar/t). In this case E'_K , measured after the expansion on the lattice, would be dominated by E_I thus allowing the observation of the interaction strength at which the MI appears in the trap.²²

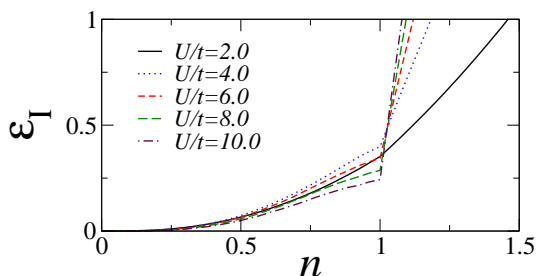


FIG. 3: (color online). Ground-state on-site interaction energy per lattice site (ϵ_I) of fermions as a function of the density [obtained from a periodic system (no trap) with 102 lattice sites], for different values of U/t . At $n = 1$ fermions are in the MI phase, and for any other value of n they are in a metallic phase.

In order for the above proposal to work, one needs a fast conversion of the interaction energy into kinetic energy. We expect this to be the case since the reduction of the density during the expansion produces a preponderance of empty and singly occupied states over the doubly occupied ones, i.e., on-site interactions get strongly suppressed. For example, in the ground state, the dependence of the on-site interaction energy on the density is shown in Fig. 3. One can see that below $n = 0.25$, the interaction energy is negligible, independent of the on-site repulsion U .

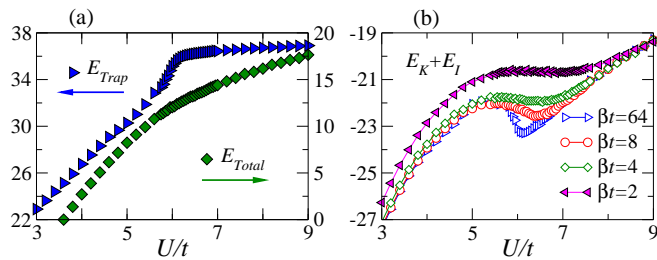


FIG. 4: (color online). (a) Trap (E_{Trap}) and total (E_{Total}) energies corresponding to the systems of Figs. 2(d)-2(f). (b) $E_K + E_I$ for systems with the same trap parameters of Fig. 2 and different inverse temperatures $\beta = 1/k_B T$. $\beta t = 64$ corresponds to the ground-state results of Figs. 2(d)-2(f).

Measuring energies to detect the formation of MI domains has the advantage of being useful independent of the statistics of the particles involved. In Figs. 2(d)–2(f), we also show results corresponding to the bosonic system in Fig. 1. The same features discussed above for fermions are present in the bosonic case. We should stress here that the minimum that signals the formation of the MI in Fig. 2(f) is an exclusive property of trapped systems, i.e., it is not present in the periodic case. This minimum is related to the fast increase of the trapping energy E_{Trap} [see Fig. 4(a)] produced by the formation of Mott domains, which push particles to the outer regions of the trap. On the other hand, as expected from the absence of a global phase transition,¹⁷ the total energy of the system increases smoothly throughout the formation of the Mott plateau [Fig. 4(a)]. Hence, we expect the above signatures to be present also in higher-dimensional systems where most of the experiments are carried out.

To what extent will finite temperatures reduce this signal? We find that as long as the temperature is low enough to allow for the formation of a MI phase, the dips in the energy are present. In Fig. 4(b), we show $E_K + E_I$ for systems at different inverse temperatures $\beta = 1/k_B T$ (where k_B is the Boltzmann constant and T is the temperature). For $\beta t = 64$, the system is essentially in its ground state [results in Figs. 2(d)–2(f)]. As seen in Fig. 4(b), the ground-state minimum of $E_K + E_I$ is still present (although weakening) with increasing temperature ($\beta t = 8$ and 4) when Mott domains are still observed in the density profiles. For high temperatures [$\beta t = 2$ in Fig. 4(b)], no Mott plateau appears in the trap and no minimum is seen in $E_K + E_I$.

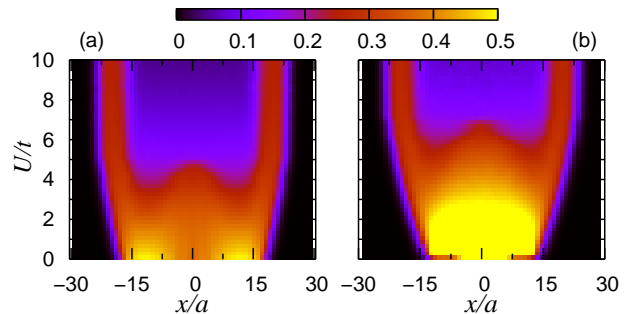


FIG. 5: (color online). Intensity plot of the density fluctuations $\Delta_i = \langle n_i^2 \rangle - \langle n_i \rangle^2$ vs position and interaction strength in fermionic (a) and bosonic (b) systems with 40 atoms on 60 lattice sites and $V_2 a^2 = 0.01t$. With increasing U , two Mott domains appear at the sides of the central metallic phase before a full Mott core develops in the center of the trap. In (b), for low values of U/t , Δ_i has been truncated as in Fig. 1.

In general, Mott-insulating plateaus can also appear on the sides of a central metallic region with $n > 1$.^{8,9,12} With increasing U , these MI regions spread inward and merge to occupy the core of the trap.^{8,9,17,18} The evolution of Δ_i for a system like this is shown in Fig. 5 for fermions and bosons with the same trap parameters. The emergence of two Mott domains around the central

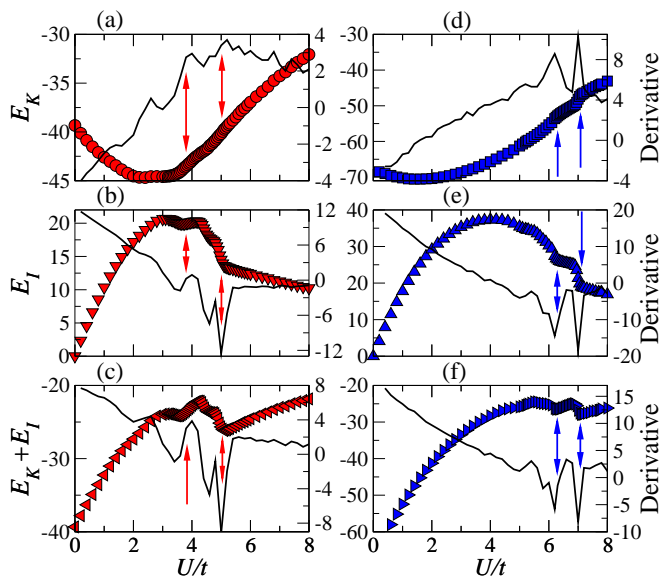


FIG. 6: (color online). (a), (d) Kinetic energy (E_K), (b), (e) interaction energy (E_I), and (c), (f) the sum $E_K + E_I$, for fermions (a-c) and bosons (d-f) in the systems of Figs. 5 (40 atoms and $V_2a^2 = 0.01t$). Continuous lines depict the numerical derivatives of the energies. The arrows indicate when two MI domains (lower value of U/t) and the MI core (larger value of U/t) emerge in each system.

metallic phase is reflected by a suppression of Δ around $U/t \sim 3.8$ for fermions (a), and $U/t \sim 6.3$ for bosons (b). The central MI core develops at $U/t \sim 5.0$ for fermions (a) and $U/t \sim 7.1$ for bosons (b).

In Fig. 6, we show the kinetic and interaction energies and their sum for fermions [(a)–(c)] and bosons [(d)–(f)]. Clear local minima can be seen in $E_K + E_I$, Figs. 6(c) and 6(f), when (i) The two MI domains of fermions (bosons) start to develop at the sides of the central metallic (superfluid) phase, and (ii) when the Mott core forms in the center of the trap due to the merging of the two Mott shoulders. An increase of $E_K + E_I$ between these two points occurs because when the two MI domains surround the central metallic (superfluid) region, the transfer of particles to the outer regions costs a finite amount of trapping energy. This produces a “freezing” of the

density profiles with increasing U so that $E_K + E_I$ increases by finite amounts before particles can be transferred out of the Mott regions to produce a full MI in the trap center.²¹ We have also found that the behavior of the energies between points (i) and (ii) depends on the trap parameters. This means that complicated structures may be observed related to the discontinuous transfer²¹ of particles out of the central metallic (superfluid) region [see for example the fermionic case in Figs. 6(b) and 6(c) in contrast to the bosonic case in Figs. 6(e) and 6(f)]. They are not related to the formation of new Mott domains. One can be certain that the full Mott plateau in the center of the trap has been formed from the smooth increase of $E_K + E_I$ with U after a minimum. (In this case, the density profiles almost do not change with U .)⁹

In Fig. 6, we have also shown the numerical derivatives of the energies. They also provide clear evidence for the formation of Mott domains. In the fermionic case, the derivative of E_K [Fig. 6(a)] decreases steadily after the full Mott insulator sets in the middle of the trap. Two very weak maxima can be also seen at the points signaled by the arrows. [They are clearer in the bosonic case, Fig. 6(b).] The two values of U/t where the derivative of $E_K + E_I$, Figs. 6(c) and 6(f), increases through zero provide a further signature of the two minima in $E_K + E_I$.

In summary, we have shown that minima in $E_K + E_I$ signal the formation of Mott domains of fermions or bosons in a trap. We have also studied the signatures that MI phases imprint in the derivatives of the kinetic and interaction energies, and of their sum. We have discussed the relevance of our findings to the detection, by means of TOF measurements, of the formation of Mott domains of fermions and bosons confined on optical lattices. Our proposal represents a novel way to detect the metal–Mott-insulator transition using TOF measurements in fermionic systems, while for bosons the implementation of our findings provides an alternative way to support the established experimental evidence of the superfluid–Mott-insulator transition.

Acknowledgments M.R. thanks T. Esslinger and R. R. P. Singh for useful discussions. This work was supported by NSF-DMR-0312261, NSF-DMR-0240918, and DE-FG02-05ER46240.

¹ M. Greiner *et al.*, Nature **415**, 39 (2002).
² T. Stöferle *et al.*, Phys. Rev. Lett. **92**, 130403 (2004).
³ G. Modugno *et al.*, Phys. Rev. A **68**, 011601(R) (2003).
⁴ H. Ott *et al.*, Phys. Rev. Lett. **92**, 160601 (2004); **93**, 120407 (2004).
⁵ M. Köhl *et al.*, Phys. Rev. Lett. **94**, 080403 (2005).
⁶ H. Moritz *et al.*, Phys. Rev. Lett. **94**, 210401 (2005).
⁷ N. F. Mott, Proc. Phys. Soc. London **A49**, 72 (1937).
⁸ M. Rigol *et al.*, Phys. Rev. Lett. **91**, 130403 (2003).
⁹ M. Rigol and A. Muramatsu, Phys. Rev. A **69**, 053612 (2004); Opt. Commun. **243**, 33 (2004).
¹⁰ G. Sugiyama and S. E. Koonin, Annals of Phys. **168**, 1

(1986).
¹¹ S. Sorella *et al.*, Europhys. Lett. **8**, 663 (1989).
¹² X.-J. Liu *et al.*, Phys. Rev. Lett. **94**, 136406 (2005).
¹³ D. Jaksch *et al.*, Phys. Rev. Lett. **81**, 3108 (1998).
¹⁴ A. W. Sandvik, J. Phys. A **25**, 3667 (1992); Phys. Rev. B **59**, R14157 (1997).
¹⁵ M. Rigol and A. Muramatsu, Phys. Rev. A **70**, 043627 (2004).
¹⁶ T. D. Kühner and H. Monien, Phys. Rev. B **58**, R14741 (1998), and references therein.
¹⁷ G. G. Batrouni *et al.*, Phys. Rev. Lett. **89**, 117203 (2002).
¹⁸ C. Kollath *et al.*, Phys. Rev. A **69**, 031601(R) (2004).

¹⁹ S. Wessel *et al.*, Phys. Rev. A **70**, 053615 (2004).

²⁰ F. Gerbier *et al.*, Phys. Rev. Lett. **95**, 050404 (2005).

²¹ P. Sengupta *et al.*, Phys. Rev. Lett. **95**, 220402 (2005).

²² We thank T. Esslinger for suggesting this possibility.